arXiv:cond-mat/0404707v1 [cond-mat.stat-mech] 29 Apr 2004

Critical adsorption and Casimir torque in wedges and at ridges

G. Palágyi[1,2,*] and S. Dietrich[1,2]

[1] *Max-Planck-Institut für Metallforschung, Heisenbergstr. 3, D-70569 Stuttgart, Germany, and*
[2] *Institut für Theoretische und Angewandte Physik, Universität Stuttgart, Pfaffenwaldring 57, D-70569 Stuttgart, Germany*

(Dated: February 2, 2008)

Geometrical structures of confining surfaces profoundly influence the adsorption of fluids upon approaching a critical point T_c in their bulk phase diagram, i.e., for $t = (T-T_c)/T_c \to \pm 0$. Guided by general scaling considerations, we calculate, within mean-field theory, the temperature dependence of the order parameter profile in a wedge with opening angle $\gamma < \pi$ and close to a ridge ($\gamma > \pi$) for $T \gtrless T_c$ and in the presence of surface fields. For a suitably defined reduced excess adsorption $\overline{\Gamma}_{\pm}(\gamma, t \to \pm 0) \sim \overline{\Gamma}_{\pm}(\gamma)|t|^{\beta-2\nu}$ we compute the universal amplitudes $\overline{\Gamma}_{\pm}(\gamma)$, which diverge as $\overline{\Gamma}_{\pm}(\gamma \to 0) \sim 1/\gamma$ for small opening angles, vary linearly close to $\gamma = \pi$ for $\gamma < \pi$, and increase exponentially for $\gamma \to 2\pi$. There is evidence that, within mean-field theory, the ratio $\overline{\Gamma}_{+}(\gamma)/\overline{\Gamma}_{-}(\gamma)$ is independent of γ. We also discuss the critical Casimir torque acting on the sides of the wedge as a function of the opening angle and temperature.

PACS numbers: 64.60.Fr, 68.35.Rh, 68.43.Fg, 61.20.-p

I. INTRODUCTION

Boundaries induce deviations of the local structural properties of condensed matter from their corresponding bulk values. Typically the width of such boundary layers is proportional to the bulk correlation length ξ. Near a continuous bulk phase transition at a temperature $T = T_c$, the correlation length diverges according to a power law $\xi_{\pm}(t = (T - T_c)/T_c \to \pm 0) = \xi_0^{\pm}|t|^{-\nu}$ with a universal bulk exponent ν and nonuniversal amplitudes $\xi_0^{\pm}$ whose ratio ξ_0^{+}/ξ_0^{-} is universal, too. For the three-dimensional Ising universality class $\nu \simeq 0.63$ and $\xi_0^{+}/\xi_0^{-} \simeq 2$ [1], whereas within mean-field theory, which is valid for spatial dimensions $d \geq 4$, $\nu = 1/2$ and $\xi_0^{+}/\xi_0^{-} = \sqrt{2}$. The nonuniversal amplitudes $\xi_0^{\pm}$ are typically in the order of the range of the interaction potential of the ordering degrees of freedom, i.e., a few Å. The correlation length is defined as the scale of the exponentially decaying two-point correlation function $\sim e^{-r/\xi}$.

The local critical properties near planar confining surfaces have been studied theoretically and experimentally in detail. It has turned out, that each bulk universality class splits up into three possible surface universality classes denoted as ordinary, special, and normal transitions. Each of them gives rise to distinct surface critical phenomena. The type of boundary conditions determines which surface universality class a given system belongs to. The ordinary transition requires the absence of surface fields, the special transition is characterized by the absence of a surface field, too, but also by suitably tuned, enhanced surface couplings between the ordering degrees of freedom, and the normal transition represents systems whose surfaces are exposed to surface fields. As indicated by the name, the latter one is the generic case. For example the normal transition applies to one-component fluids near their liquid-vapor critical point, or to binary liquid mixtures near their demixing critical point. In both cases the substrate potential of the confining container walls and the missing interactions due to the fact that the fluid particles cannot penetrate the substrate give rise to the effective surface fields acting on the corresponding order parameter (density or concentration difference). As a consequence, in this case even above T_c there is a nonvanishing order parameter profile, which decays to zero for $T \geq T_c$ upon approaching the bulk, i.e., for increasing normal distance $z \to \infty$ from the surface at $z = 0$. For $T < T_c$ this profile attains the nonzero value of the bulk order parameter for $z \to \infty$. Following early calculations on magnetic systems by K. Binder and P. C. Hohenberg [2], this so-called critical adsorption was first examined in detail by Fisher and de Gennes [3] and has since been analyzed for many systems both theoretically [4, 5, 6] and experimentally [7], and a fair agreement between theory and experiment has been found [8, 9].

Surface order above the bulk critical temperature can also be due to spontaneous symmetry breaking caused by enhanced surface couplings between the ordering degrees of freedom, e.g. spins in magnetic systems. The transition to this state from the disordered state is usually denoted as the extraordinary transition. Bray and Moore [10] predicted an equivalence between the normal and the extraordinary transitions that was later proved by Burkhardt and Diehl [11]. In contrast to the ordinary transition in magnetic systems, the corresponding extraordinary transition has been investigated to a lesser extent. Extending and improving earlier work [12, 13, 14, 15], Diehl and Smock [16] have carried out a field-theoretic renormalization-group calculation in $4-\epsilon$ dimensions for the extraordinary transition in semi-infinite systems belonging to the Ising universality class

*Electronic address: palagyig@almos.vein.hu; Permanent address: Department of Physics, University of Veszprém, H-8201 Veszprém, POBox 158, Hungary

[17] computing the order parameter profile to one-loop order. The results are in fair agreement with those obtained by Monte Carlo simulations [9].

These studies are devoted to the case of planar surfaces. Only very carefully treated solid surfaces are atomically flat; generically, however, they exhibit corrugations. Besides these random deviations from the flat topography, there is nowadays an abundance of experimental techniques [18] that allow one to endow solid surfaces with precise lateral geometrical structures, ranging from the μm scale down to tens of nm. Inter alia, such solid surfaces are used within the context of microfluidic devices [19] in order to guide fluids along such structures. The fluids perfectly fill this laterally structured environment and thus fully exhibit the strong structural changes associated with that. In this context it is of interest what kind of structures appear in the fluid if it is brought, say, close to a demixing transition and is exposed to geometrically structured substrates. If the characteristic sizes of the lateral structures are comparable with the correlation length, which in fluids reaches typically up to a few thousand Å close to T_c, one can expect a strong influence on the aforementioned critical adsorption phenomena.

Theoretically this raises the issue of how the local critical properties depend on the *shape* of the boundaries. A typical manmade structure is a series of grooves with various shapes of the cross section, e.g. wedgelike. The first step in their investigation is the study of a single wedge, which already shows new features and gives new insight into the influence of geometry on critical behavior. The ordinary transition of the isotropic N-vector model at an edge has been investigated by Cardy [20] within the framework of mean-field theory, the renormalization group, and ϵ-expansion. Subsequently the two-dimensional wedge (corner geometry) was studied by exact calculations, mainly for Ising models [21], and by conformal mapping at the bulk critical temperature [22]. New edge and corner exponents were found that depend on the opening angle γ of the wedge. More recently similar findings of Monte Carlo simulations of the ordinary transition of the three-dimensional Ising model [23] have been reported, in accordance with high temperature series expansions [24]. The angle dependence of the critical wedge exponents can be attributed to the fact that the wedge geometry lacks a length scale and thus is invariant under rescaling. The opening angle is therefore a marginal variable in a renormalization transformation, and *may* enter into the expressions for the exponents. The same will happen for all other scale-invariant shapes of the boundaries [25]. However, for a given opening angle, the values of the critical exponents are expected to be universal and independent of microscopic details. According to recent Monte Carlo simulations of three-dimensional Ising models with edges and corners [26], angle dependent critical exponents are observed at the ordinary transition, whereas the surface transition seems to be nonuniversal. The critical exponents in this latter case appear to depend on the strengths of the local couplings, in analogy with exact results obtained for the two-dimensional Ising model with defect lines [27]. Critical adsorption has also been studied in general dimensions d on curved surfaces [28].

Since critical adsorption changes the composition of a binary liquid mixture close to its surface, mechanical properties, such as the local viscosity and the mutual diffusion coefficient will also vary in space. So we expect various phenomena, such as flow properties in porous media, the spreading properties of droplets, surface chemical reactions, the permeability of membranes etc. [29], to be influenced significantly by critical adsorption.

Critical adsorption in a wedge has been studied by Hanke et. al. [30]. Within mean-field theory the order parameter profile was calculated exactly *at* the critical point. Through an interpolation scheme between exact results in $d = 2$ and the mean-field results corresponding to $d = 4$, angle dependent critical exponents of the order parameter and those governing the decay of two-point correlation functions were obtained for $d = 3$ as well. The present study extends these investigations into various directions.

First, we analyze the temperature dependence off criticality for critical adsorption in a wedge. General scaling properties for the order parameter profile and the excess adsorption are discussed and the corresponding scaling functions are calculated within mean-field theory. This analysis is carried out above and below T_c, including a systematic study of the dependence on the opening angle γ of the wedge. This covers also the case $\gamma > \pi$ describing critical adsorption near a ridge.

Second, as a new feature, we study the Casimir torque acting on the sides of the wedge or ridge. The confinement modifies the fluctuation spectrum of the critical fluctuations and the order parameter profiles. This leads to a dependence of the free energy of the critical medium on the shape of and the distance between the confining boundaries, which results in an effective force acting on them. Thus the physical origin of this force, originally predicted by Fisher and de Gennes [3] for two parallel plates immersed into a binary liquid mixture near its continuous demixing transition, is analogous to the Casimir force acting on conducting plates in vacuum due to the confinement of quantum mechanical vacuum fluctuations of the electromagnetic field [31]. The Casimir force is governed by universal scaling functions [32] and is superimposed on the noncritical background forces, which in the case of fluids are given by dispersion forces. Recent experiments [33] have confirmed corresponding theoretical predictions for the plate geometry [34]. For curved surfaces the critical Casimir force plays an important role in the flocculation of colloidal particles suspended in a solvent undergoing a continuous phase transition [35]. In the present context the free energy of the critical medium depends on the opening angle γ; its derivative with respect to γ amounts to the critical Casimir torque acting on the sides of the wedge or ridge. If the substrate forming the wedge or ridge is composed of soft materials like,

e.g., membranes, this critical Casimir torque is expected to give rise to elastic deformations. It might also be experimentally accessible by suitable force microscopy with moveable sidewalls of a wedgelike structure.

The paper is organized as follows. In Sec. II we discuss the general scaling properties of the order parameter profiles and the excess adsorption. The scaling functions are determined within mean-field theory and analyzed in detail in Sec. III. Section IV focuses on the free energy of the confined fluid and the critical Casimir torque resulting from its angle dependence. Section V summarizes our findings. In the Appendix we discuss how the excess adsorption in a wedge or at a ridge decomposes into surface and line contributions with two possible experimental realizations.

II. GENERAL SCALING PROPERTIES OF ORDER PARAMETER PROFILES AND EXCESS ADSORPTION

Since fluids can fill a container of arbitrary shape, in the present context of critical systems exposed to substrates shaped as wedges we consider *fluids* close to their bulk critical point T_c. This can be either a liquid-vapor critical point or a demixing critical point in the case of binary liquid mixtures. The interaction of the container walls with the fluid particles results in a spatial variation of the number densities close to the boundaries. The deviation of the density of the fluid, or of the concentration of one of its two components in the case of binary liquid mixtures, from the corresponding bulk value at T_c is chosen as the local order parameter describing the phase transition.

The order parameter profile $m_\pm^{\infty/2}(\zeta,t)$ near a *planar* interface and close to the critical temperature T_c takes the following scaling form [8, 9, 14, 16, 36]:

$$m_\pm^{\infty/2}(\zeta,t) = a|t|^\beta P_\pm^{\infty/2}(\zeta/\xi_\pm),\ \ t=(T-T_c)/T_c, \quad (1)$$

for distances $\zeta \gtrsim \sigma$ perpendicular to the interface and sufficiently large compared to a typical microscopic length σ. $\xi_\pm(t\to 0) = \xi_0^\pm |t|^{-\nu}$ is the bulk correlation length above $(+)$ or below $(-)$ T_c, β and ν are the standard bulk critical exponents, and t is the reduced temperature. The scaling functions $P_\pm^{\infty/2}(\zeta_\pm = \zeta/\xi_\pm)$ are universal once the nonuniversal bulk amplitudes a and $\xi_0^\pm$ are fixed, where a is the amplitude of the bulk order parameter $m_-^{\infty/2}(\zeta=\infty, t\to 0^-) = a|t|^\beta = m_b(t)$. With the prefactors $\xi_0^\pm$ fixed as those of the *true* correlation length defined by the exponential decay of the bulk two-point correlation function in real space, one finds $P_-^{\infty/2}(\infty)=1$, $P_+^{\infty/2}(\infty)=0$, $P_-^{\infty/2}(\zeta_-\to\infty)-1 \sim e^{-\zeta_-}$, $P_+^{\infty/2}(\zeta_+\to\infty)\sim e^{-\zeta_+}$ and $P_\pm^{\infty/2}(\zeta_\pm\to 0) = c_\pm \zeta_\pm^{-\beta/\nu}$ [16], so that

$$m^{\infty/2}(\zeta, t=0) = a c_\pm (\zeta/\xi_0^\pm)^{-\beta/\nu}. \quad (2)$$

Any other choice for the definition of the correlation length leads to a redefinition of the scaling functions $P_\pm^{\infty/2}$ such that all observable quantities remain unchanged. This underscores that the scaling functions are universal, but that their form depends on the definition of the correlation length. The amplitudes of the scaling functions are fixed by the requirement $P_-^{\infty/2}(\infty)=1$. Accordingly the numbers $c_\pm$ are universal surface amplitudes which are definition-dependent [8].

Close to T_c the total enrichment at the interface of, say, the A particles as compared to the B particles of a binary liquid mixture is given by the excess adsorption, which is an experimentally accessible integral quantity. For a planar surface, one has

$$\Gamma_\pm^{\infty/2}(t) = \int_0^\infty [m_\pm^{\infty/2}(\zeta,t) - m_\pm^{\infty/2}(\zeta=\infty,t)]d\zeta \quad (3)$$

The scaling behavior of $\Gamma_\pm^{\infty/2}(t)$ has been discussed in Ref. [8] in detail. The ζ integration can be split into the intervals $\zeta>\sigma$ and $0\le\zeta\le\sigma$, and for large ζ the order parameter profile $m_\pm^{\infty/2}(\zeta,t)$ can be replaced by Eq. (1), which gives

$$\Gamma_\pm^{\infty/2}(t) = \int_0^\sigma [m_\pm^{\infty/2}(\zeta,t) - m_\pm^{\infty/2}(\zeta=\infty,t)]d\zeta + a\xi_0^\pm |t|^{\beta-\nu}\int_{\sigma/\xi_\pm}^\infty [P_\pm^{\infty/2}(\zeta_\pm) - P_\pm^{\infty/2}(\zeta_\pm=\infty)]d\zeta_\pm. \quad (4)$$

Upon approaching T_c the first integral remains finite and yields a nonuniversal constant, which is subdominant to the diverging second term. The second integral leads to the well known power-law singularity of $\Gamma_\pm^{\infty/2}(t\to 0)$ for $d<4$:

$$\Gamma_\pm^{\infty/2}(t\to 0) = a\xi_0^\pm g_\pm \frac{|t|^{\beta-\nu}}{\nu-\beta}, \qquad d<4, \quad (5)$$

where the numbers $g_\pm$ are universal with their values depending on the definitions of the bulk order parameter and the correlation length. In $d=4$ one finds upon inserting the mean-field expression for $P_\pm^{\infty/2}$ (see Ref. [16]) into Eq. (4) that $\Gamma_\pm^{\infty/2}(t)$ diverges logarithmically. This result can be reconciled with Eq. (5) by noting that $\Gamma_\pm^{\infty/2}$ actually needs additive renormalization leading to [8]

$$\Gamma_\pm^{\infty/2}(t\to 0) = a\xi_0^\pm g_\pm \frac{|t|^{\beta-\nu}-1}{\nu-\beta}, \qquad d\le 4. \quad (6)$$

In the *wedge or ridge geometry* (Fig. 1) the order parameter profile depends on the radial distance r from the apex, on the polar angle θ, and on the opening angle γ, so that the variation of the profile is two-dimensional with

corresponding generalized scaling functions:

$$m_\pm(\boldsymbol{r},t;\gamma) = a|t|^\beta P_\pm(r/\xi_\pm,\theta;\gamma). \tag{7}$$

As before, the scaling functions are universal once the

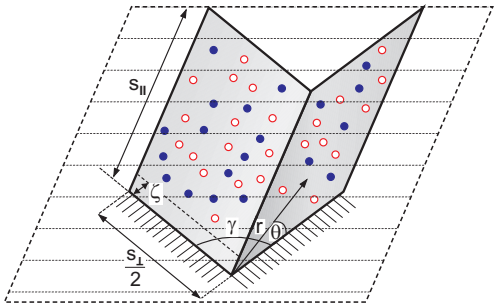

wedge

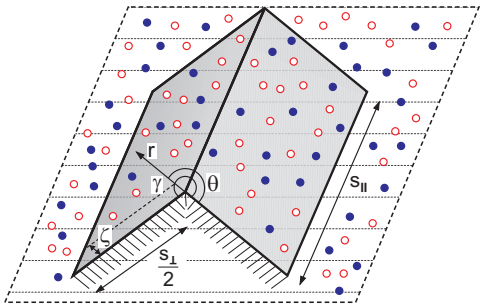

ridge

FIG. 1: A wedge and a ridge with opening angle γ exposed to a binary liquid mixture. The system is translationally invariant in the subspace parallel to the edge. Within a plane orthogonal to the edge the polar coordinates are r and θ. The linear extensions of the confining surfaces are $s_\parallel$ and $s_\perp$.

nonuniversal bulk amplitudes a and $\xi_0^\pm$ are fixed, where a is the amplitude of the bulk order parameter and the amplitudes $\xi_0^\pm$ are prefactors of the *true* correlation length as in the case of the infinite planar wall. One finds [30] with $r_\pm = r/\xi_\pm$ that $P_-(r_- = \infty,\theta) = 1$, $P_+(r_+ = \infty,\theta) = 0$, $P_-(r_- \to \infty,\theta) - 1 \sim e^{-\sin(\theta) r_-}$ $(\theta < \gamma/2)$, $P_+(r_+ \to \infty,\theta) \sim e^{-\sin(\theta) r_+}$ $(\theta < \gamma/2)$, $P_\pm(r_\pm \to 0,\theta) = \tilde{c}_\pm(\theta,\gamma) r_\pm^{-\beta/\nu}$, and

$$\begin{aligned} P_\pm(r_\pm, \theta \to 0) &= c_\pm \zeta_\pm^{-\beta/\nu} \\ &= c_\pm (r_\pm \sin\theta)^{-\beta/\nu}, \end{aligned} \tag{8}$$

where $\zeta_\pm = r_\pm \sin\theta$ (see Fig. 1). The amplitudes of the scaling functions are again fixed by the requirement $P_-(r = \infty,\theta) = 1$. The numbers $c_\pm$ are the universal surface amplitudes of the scaling function of the infinite planar wall [Eq. (2)], and $\tilde{c}_\pm(\theta,\gamma)$ are universal functions. Both $c_\pm$ and $\tilde{c}_\pm$ depend on the definition of the correlation length. The scaling functions also reflect the symmetry of present the geometry:

$$P_\pm(r_\pm,\theta;\gamma) = P_\pm(r_\pm,\gamma-\theta;\gamma). \tag{9}$$

We define the *excess* adsorption for this geometry confined by surfaces of linear extensions $s_\perp$ in the plane perpendicular to the edge and $s_\parallel$ in the translationally invariant directions (see Fig. 1) as

$$\tilde{\Gamma}_\pm(s_\perp, s_\parallel, t;\gamma) = \int_V d^d r [m_\pm(\boldsymbol{r},t;\gamma) - m_b(t)], \tag{10}$$

where the integral is taken over a macroscopic volume V occupied by the liquid. According to the Appendix this excess adsorption decomposes into a surface contribution that scales with the actual surface area of the confining walls $(s_\perp s_\parallel^{(d-2)})$ and a line contribution that scales with the extension in the invariant directions $(s_\parallel^{(d-2)}$, i.e., a line in $d = 3)$ [37]:

$$\begin{aligned} \tilde{\Gamma}_\pm(s_\perp, s_\parallel, t;\gamma) \;&=\; \Gamma_s^\pm(t) s_\perp s_\parallel^{(d-2)} + \Gamma_l^\pm(t,\gamma) s_\parallel^{(d-2)} \\ &\quad + \mathcal{O}(s_\perp^{-1}). \end{aligned} \tag{11}$$

While the surface term is determined solely by the order parameter profile of a semi-infinite binary mixture exposed to a flat substrate, the line contribution is the specific contribution arising from the change of the order parameter profile caused by the edge. Due to the symmetry of the system one can determine the amplitudes $\Gamma_s^\pm$ and $\Gamma_l^\pm$ for the wedge and the ridge explicitly by considering only one half of the wedge or the ridge [see Eq. (9)], and by suitably subtracting and adding the order parameter profile $m_\pm^{\infty/2}(\zeta = r\sin\theta, t)$ of a fluid in contact with an infinite planar wall in the integrand of Eq. (10) (compare Eqs. (3)-(6) and the Appendix):

$$\Gamma_s^\pm(t) = \Gamma_\pm^{\infty/2}(t) \tag{12}$$

and

$$\begin{aligned} \Gamma_l^\pm(t,\gamma) \;&=\; 2\int_0^{\gamma/2} d\theta \int_0^\infty dr\, r [m_\pm(r,\theta,t;\gamma) \\ &\quad - m_\pm^{\infty/2}(\zeta(r,\theta),t)]. \end{aligned} \tag{13}$$

Based on Eq. (7) $\Gamma_l^\pm(t,\gamma)$ takes on the scaling form

$$\Gamma_l^\pm(t,\gamma) = a\xi_0^{\pm\,2} |t|^{\beta-2\nu} \overline{\Gamma}_\pm(\gamma) \tag{14}$$

with the universal amplitude functions

$$\begin{aligned} \overline{\Gamma}_\pm(\gamma) \;&=\; 2\int_0^{\gamma/2} d\theta \int_0^\infty dr_\pm\, r_\pm [P_\pm(r_\pm,\theta;\gamma) \\ &\quad - P_\pm^{\infty/2}(\zeta_\pm(r_\pm,\theta))] \end{aligned} \tag{15}$$

where $\zeta_\pm(r_\pm,\theta) = r_\pm \sin\theta$. We note that the integral in Eq. (15) is finite for $d = 4$, i.e., $\overline{\Gamma}_\pm$ does not carry a factor

proportional to $\frac{1}{\nu-\beta}$ as $\Gamma_{\pm}^{\infty/2}$ does (compare Eq. (6)). As one can see from Eqs. (6) and (14), the subdominant line contribution to the excess adsorption carries a more singular temperature dependence than the leading planar surface term. Thus the scaling properties of the order parameter profile completely fix the functional form of the excess critical adsorption up to the dependence of the universal amplitudes $\overline{\Gamma}_{\pm}(\gamma)$ on the opening angle. Since this dependence cannot be inferred from general scaling arguments, it must be determined explicitly. This will be carried out within mean-field theory in the following section. This is possible because as stated above $\overline{\Gamma}_{\pm}(\gamma)$ is finite for $d = 4$.

III. SCALING FUNCTIONS WITHIN MEAN-FIELD THEORY

A. Order parameter profiles

The standard Ginzburg-Landau Hamiltonian for describing critical phenomena in confined geometries is [4, 5]

$$H\{\phi\} = \int_{V_{w(r)}} dV \left\{ \frac{1}{2}(\nabla\phi)^2 + \frac{\tau}{2}\phi^2 + \frac{u}{24}\phi^4 \right\}, \quad (16)$$

with a scalar order parameter field $\phi(\boldsymbol{r})$, supplemented by the boundary condition $\phi = +\infty$ at the surfaces of the wedge (ridge) corresponding to the critical adsorption fixed point [11]. The parameter τ is proportional to the reduced temperature t, u is the coupling constant, and the integration runs over the volume $V_{w(r)}$ of the wedge (ridge) (see Fig. 1). Within mean-field theory $\tau = t/(\xi_0^+)^2$ for $T > T_c$, and $\tau = -\frac{1}{2}|t|/(\xi_0^-)^2$ for $T < T_c$ with $\xi_0^+/\xi_0^- = \sqrt{2}$.

After functional minimization one obtains for the order parameter $m = \sqrt{u/12} < \phi >$ the differential equation

$$\Delta m = \tau m + 2m^3, \quad (17)$$

where $m = m(r, \theta, \tau; \gamma)$. Since the scaling functions in Eq. (1) have the limiting behavior shown in Eq. (2), where $\beta = \nu = 1/2$ within the mean-field approximation, in order to derive a boundary condition for the numerical calculation of the order parameter close to the surfaces of the wedge, i.e., $\theta \to 0$ for r fixed, we seek a solution for Eq. (17) in the form

$$m(r, \theta, \tau) = \frac{A(r,\tau)}{\theta} + B(r,\tau) + C(r,\tau)\theta + D(r,\tau)\theta^2 + \mathcal{O}(\theta^3) \quad (18)$$

for $\theta \ll 1$ (suppressing the γ-dependence in the notation) and obtain for both $\tau > 0$ and $\tau < 0$

$$m(r, \theta, \tau) = \frac{1}{r}\frac{1}{\theta} + \left(\frac{1}{6r} - \frac{\tau r}{6}\right)\theta + \mathcal{O}(\theta^3) \quad (19)$$

($B(r,\tau) \equiv 0$, $D(r,\tau) \equiv 0$). This result agrees with the direct expansion of the mean-field profile obtained for $\tau = 0$ [30]. In terms of the scaling functions $P_{\pm}$ this implies [see Eq. (8)]:

$$P_+(r_+, \theta \to 0) = c_+ \frac{1}{r_+ \sin\theta}\left[1 - \frac{1}{6}r_+^2\theta^2 + \mathcal{O}(\theta^4)\right] \quad (20a)$$

$$P_-(r_-, \theta \to 0) = c_- \frac{1}{r_- \sin\theta}\left[1 - \frac{1}{12}r_-^2\theta^2 + \mathcal{O}(\theta^4)\right] \quad (20b)$$

with $c_+ = \sqrt{2}$ and $c_- = 2$ [8].

We use a numerical method [35, 38] to minimize Eq. (16) with respect to the order parameter profile at a fixed temperature, which is then subsequently varied. For computational purposes we choose suitably shaped finite volumes $V_{w(r)}$ for different opening angles γ of the wedge (w) or ridge (r). We refrain from describing this choice of volumes here, because it does not matter in the calculation of the universal amplitude functions $\overline{\Gamma}_{\pm}(\gamma)$. The choice of the volume is relevant only for that line contribution to the excess adsorption that depends only on the order parameter profile close to an infinite planar wall and thus is independent of the opening angle of the wedge (see the Appendix). As the temperature is changed we rescale the size of the volume $V_{w(r)}$ in accordance with the change of the correlation length $\xi = \xi_0 t^{-\nu}$. This way we control the finite size effects caused by the finiteness of $V_{w(r)}$ dictated by computational necessity. The finite size effects manifest themselves even close to those boundaries of the chosen volume that are far away from the walls of the wedge because of using approximate boundary conditions at these boundaries (see below). By effectively increasing the *rescaled* volume upon approaching T_c, the values of the profiles at fixed spatial points within this rescaled volume converge to a limiting value.

We choose a two-dimensional grid (i, j) and calculate the deviation of the order parameter profile from the known profile at $T = T_c$ at the given grid points. The profile near the confining surfaces of the wedge (ridge) is fixed according to Eq. (19). (The grid points are lined up parallel to the walls of the wedge.) At the surfaces of the finite volume $V_{w(r)}$ that are further away from the walls of the wedge, we prescribe initial values of the profile. Keeping these values fixed we then calculate new values of the profile inside the volume using the method of steepest descent. Having obtained the new values for the profile close to these surfaces, we change the profile at these surfaces proportionally to the change in their neighborhood, if it changes significantly in the direction perpendicular to the surfaces (the general case), or set it equal to that in neighboring layers if the profile is approximately constant close to these surfaces (for example far away from the edges of the wedges parallel to the confining walls of the wedge). The rules for the iteration according to the method of steepest descent in the space

of the parameters

$$a_{ij} = m(r_{ij}, \theta_{ij}, 0) - m(r_{ij}, \theta_{ij}, \tau) \tag{21}$$

are

$$a_{ij}^{(n+1)} = a_{ij}^{(n)} - \kappa \left. \frac{\partial H(a_{ij})}{\partial a_{ij}} \right|_{a_{ij}^{(n)}} \tag{22}$$

where κ is a convergence parameter. With this method it is not necessary to calculate the Hamiltonian itself but only its derivative. The method has been described in detail in Refs. [35] and [38], so here we only want to point out that the divergence of the profile close to the walls of the wedge causes a divergence in the derivative of the Hamiltonian, too. This can be avoided, if one takes into account the known form of the divergence of the profile close to the edges of the wedge [see Eq. (19)]. To this end we write a_{ij} as a product of two terms, one of which we choose to be such that when multiplied by the profile close to the boundaries (in the calculation of the derivative) it cancels the divergences of the profiles [see Eq. (19)], yielding a smooth gradient in the parameter space. We approximate the integrand of the gradient of $H\{\phi\}$ [see Eq.(16)] by a sum of delta-functions positioned at the grid points, so that the integral reduces to a simple sum over these points; for each opening angle κ is optimized separately for best convergence.

The scaling function of the order parameter profile in a wedge [see Eqs. (7)-(9)] with an opening angle of 90° is shown in Figs. 2-5. One can easily see that the contour

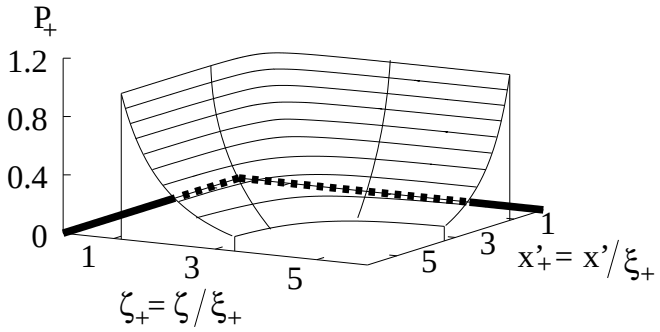

FIG. 2: The scaling function P_+ of the order parameter profile in a wedge of opening angle $\gamma = \pi/2$ with the edge located at the back of the figure at $x' = \zeta = 0$ $\{x' = r\cos\theta,\ \zeta = r\sin\theta$ [see Figs.1 and 14(a)]$\}$. The positions of the walls of the wedge coincide with the coordinate axes as indicated here with broad lines. The values of P_+ at which contour lines are drawn are multiples of 0.1 and range from 0.1 to 1.0.

lines quickly become parallel to the walls of the wedge as we move away from the edge (see Figs. 2 and 3). This is especially apparent as we approach the walls. As one moves along the bisector of the wedge, the maximal curvature κ of the contour lines decreases sharply (Fig. 3). This underscores that in terms of the *rescaled* variables, to a good approximation the effects of the edges are spatially localized. The maximal curvature κ depends linearly on the values of P_+ corresponding to the contour lines within the range of P_+ values analyzed in Fig. 3.

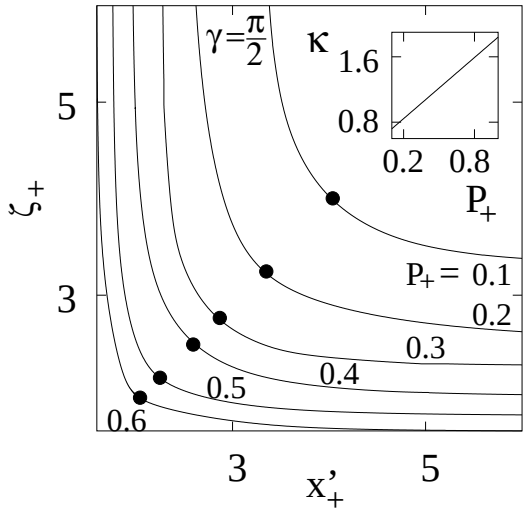

FIG. 3: Projection of the contour lines of the scaling function P_+ of the order parameter profile in a wedge of opening angle $\gamma = \pi/2$ onto the (x'_+, ζ_+) plane. The edge is located at $x'_+ = \zeta_+ = 0$. The curves correspond to values of P_+ ranging from 0.1 to 0.6 with an increment of 0.1 from top to bottom. The inset shows that the maximal curvature κ of the contour lines, occurring on the bisector (•), depends linearly on the values of P_+ corresponding to the contour lines within the range of P_+ values considered here.

Along radial directions, i.e., for $\theta = const.$ (Fig. 4) the scaling function exhibits a power law limiting behavior close to the walls in accordance with Eq. (8) and the paragraph preceding it. For large $r_\pm$ the behavior crosses over into an exponential decay: $P_+(r_+ \to \infty, \theta; \gamma) = A_+(\theta, \gamma) e^{-r_+ \sin\theta}$, $P_-(r_- \to \infty, \theta; \gamma) - 1 = A_-(\theta, \gamma) e^{-r_- \sin\theta}$, where near the walls $A_\pm$ reduce to the amplitudes of the exponential decay away from an infinite planar wall: $A_+(\theta \to 0, \gamma) = \sqrt{8}$ and $A_-(\theta \to 0, \gamma) = 2$. The dependence of $A_\pm(\theta, \gamma)$ on θ is weak. The latter values are valid for $\theta \lesssim 30°$, beyond which the prefactors of the exponential functions increase with θ. Upon approaching the walls of the wedge vertically, i.e., for $\theta \to 0$ or γ with $r_\pm$ fixed [see Eq. (8) and Fig. 5] the divergence of the profile has a power law form.

The limiting behaviors of the scaling functions $P_\pm$ close to the edge of the wedge ($r_\pm \to 0$) are described by the amplitude functions $\tilde{c}_\pm(\theta, \gamma)$ [see the paragraph following Eq. (7) and Fig. 4]:

$$P_\pm(r_\pm \to 0, \theta) = \tilde{c}_\pm(\theta, \gamma) r_\pm^{-\beta/\nu}. \tag{23}$$

These functions are plotted for $\gamma = \pi/2$ in Fig. 6. According to Eq. (8), close to the walls of the wedge, i.e., for $\theta \to 0$ these functions are given by $\tilde{c}_\pm(\theta \to 0, \gamma) = c_\pm (\sin\theta)^{-\beta/\nu}$.

The scaling function of the order parameter profile at

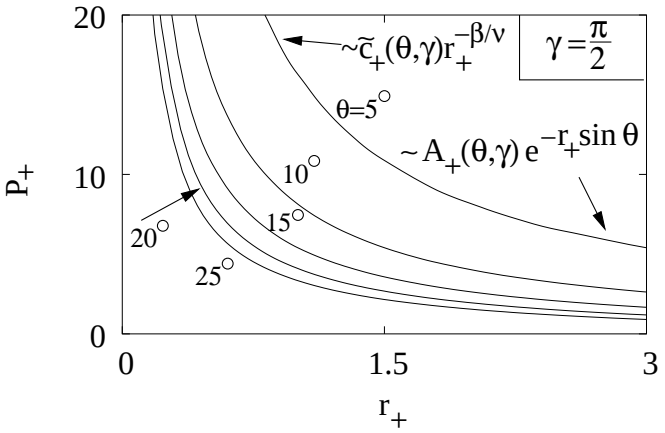

FIG. 4: The scaling function P_+ of the order parameter as a function of the distance r_+ from the edge of a wedge of opening angle $\gamma = \pi/2$. The curves correspond to values of θ ranging from 5° to 25° with an increment of 5° from top to bottom.

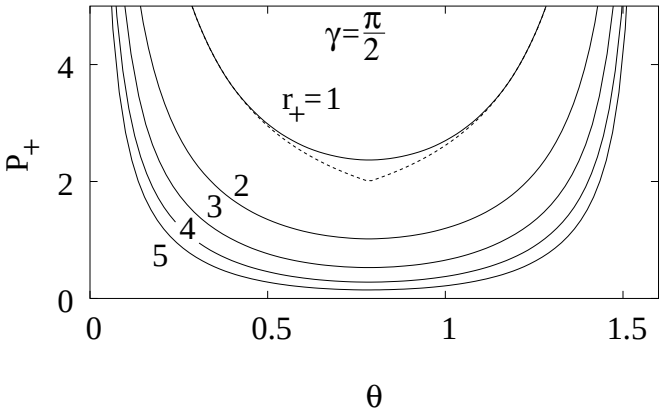

FIG. 5: The scaling function P_+ of the order parameter along arcs of different radii r_+ centered at the edge of a wedge of opening angle $\gamma = \pi/2$. The curves correspond to values of r_+ from 1 to 5 with increments of 1 from top to bottom. The curves are symmetric around $\theta = \gamma/2 = \pi/4$ and diverge as $(c_+ r_+^{-\beta/\nu})\theta^{-\beta/\nu}$ for $\theta \to 0$. For $r_+ = 1$ the comparison with the asymptotic behavior $c_+(r_+ \sin\theta)^{-\beta/\nu}$ for $\theta < \gamma/2$ and $c_+[r_+ \sin(\gamma - \theta)]^{-\beta/\nu}$ for $\theta > \gamma/2$ is shown as a dashed curve [see Eq. (8)].

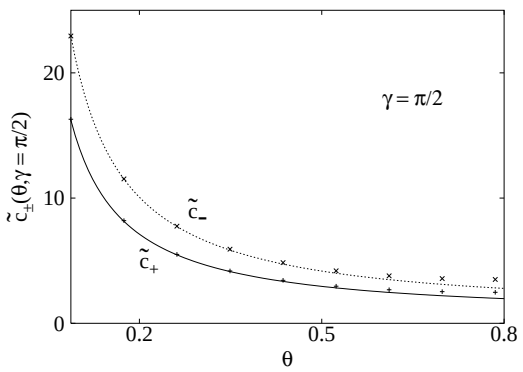

FIG. 6: The amplitude functions $\tilde{c}_\pm(\theta, \gamma = \pi/2) = \left[P_\pm(r_\pm, \theta) r_\pm^{\beta/\nu}\right]\Big|_{r_\pm \to 0}$ in a wedge of opening angle γ ($t > 0$: +, $t < 0$: ×). The solid line corresponds to the function $c_+(\sin\theta)^{-\beta/\nu}$ ($t > 0$) [see Eq. (8)] and the dotted line to $c_-(\sin\theta)^{-\beta/\nu}$ ($t < 0$), which are valid in the asymptotic regime $\theta \to 0$, but provide a surprisingly good description throughout the whole angle range $0 < \theta < \pi/4 \simeq 0.785$.

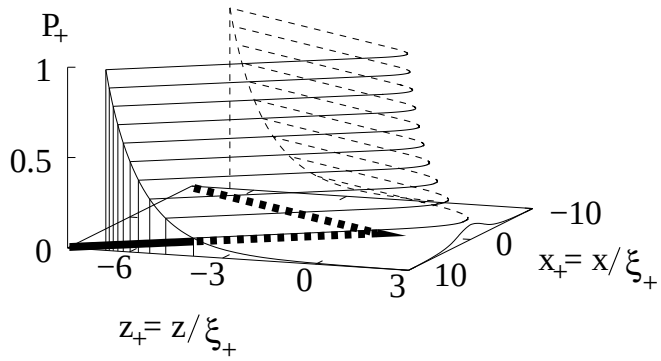

FIG. 7: The scaling function P_+ of the order parameter profile at a ridge of opening angle $\gamma = 260°$ with the edge perpendicular to the (x_+, z_+) plane and located at $x_+ = z_+ = 0$ [see Figs. 1 and, c.f., 14(b)]. The positions of the walls of the ridge are indicated here with broad lines. The values of P_+ at which contour lines are drawn are multiples of 0.1 and range from 1.0 to 0.1 (top to bottom).

a ridge [see Eqs. (7)-(9)] with an opening angle of 260° is shown in Figs. 7 and 8. One can easily see that the contour lines rapidly become parallel to the walls of the ridge as one moves along them further away from the edge. As one moves along the bisector of the ridge away from the edge, the maximal curvature κ of the contour lines decreases (Fig. 8). κ depends linearly on the values $P_\pm$ characterizing the contour lines and thus has similar limiting behaviors close to the edge of the ridge and far from it as a function of $r_\pm$, at least within the range studied in the inset of Fig. 8.

Comparing the order parameter profiles in a wedge or at a ridge with the profile near a planar wall, one can visualize the wedge or ridge as being formed by breaking the planar wall into two halves, which in the case of a wedge are brought closer to each other, and in the case of the ridge are taken further apart. Close to the edge of the wedge this increases the values of the profiles, while close to the edge of a ridge these values are decreased as compared to the profile near a planar wall.

B. Excess adsorption

The presentation of the full order parameter distribution requires to keep track of four variables: r, θ, t, and γ. Therefore it is advantageous to consider also the excess

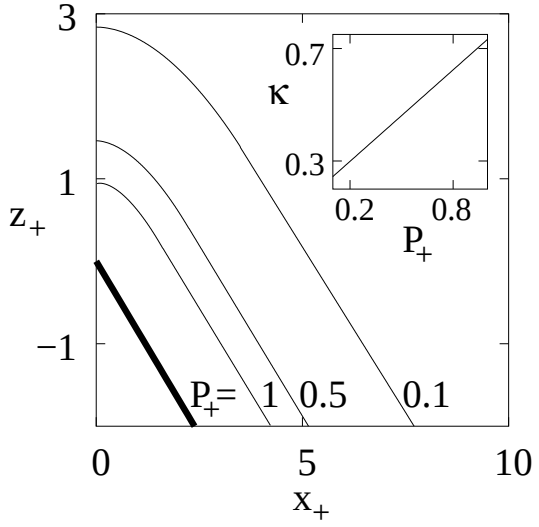

FIG. 8: Projection of the contour lines of the scaling function P_+ of the order parameter profile in a ridge of opening angle $\gamma = 260^\circ$ onto the (x_+, z_+) plane. The projection is shown only on one side of the bisector of the ridge, which coincides here with the z_+ axis. The wall of the ridge is indicated with a broad line. The edge is located at $x_+ = z_+ = 0$. The curves correspond to $P_+ = 0.1$, 0.5, and 1.0 from top to bottom. The inset shows that the maximal curvature κ of the contour lines occurring on the bisector is a linear function of P_+ within the range considered here.

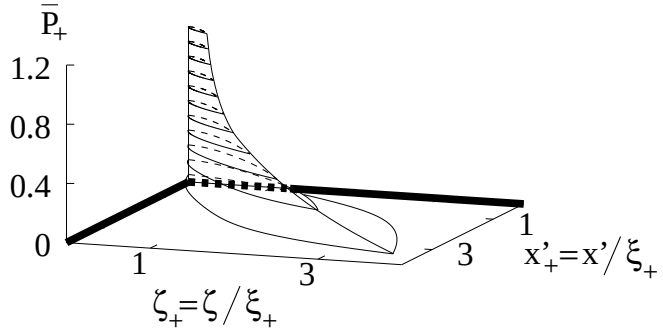

FIG. 9: Contour levels of the integrand of the integral that determines the amplitude of the reduced excess adsorption for $T > T_c$ [see Eqs. (15) and 24] in a wedge of opening angle $\gamma = \pi/2$ with the edge located at the back of the figure at $x' = \zeta = 0$ ($x' = r\cos\theta$, $\zeta = r\sin\theta$). The walls of the wedge, indicated by broad lines, coincide with the coordinate axes. The values of $\overline{P}_+$ at which contour lines are drawn increase with multiples of 0.1 and range from 0.05 to 1.05.

adsorption in wedges and at ridges, which is experimentally relevant and provides reduced information depending only on t and γ [Eq. (10)]. We are particularly interested in the line contribution [see Eqs. (11) and (13)] characterizing the effect of the wedge (ridge) geometry via its universal amplitude functions [Eq. (15)]. In order to calculate this quantity we use the fact that the integral in Eq. (15) can be rewritten as

$$\overline{\Gamma}_\pm(\gamma) = \int_0^\infty F(\overline{P}_\pm) d\overline{P}_\pm, \qquad (24)$$

where $F(\overline{P}_\pm)$ is the area enclosed by the contour lines of $\overline{P}_\pm = P_\pm(r_\pm, \theta; \gamma) - P_\pm^{\infty/2}(\zeta_\pm(r_\pm, \theta))$ (see Fig. 9). Based on these areas one is left with a one-dimensional integration to obtain $\overline{\Gamma}_\pm$ numerically. Furthermore, exploiting the observation that the geometrical shapes formed by the contour lines are similar to one another for small and large areas, respectively, and using the limiting behavior of the scaling functions, we approximate $F(\overline{P}_\pm)$ for small values of $\overline{P}_\pm$ in terms of powers of $\overline{P}_\pm$, and for large $\overline{P}_\pm$ in term of powers of $\ln(\overline{P}_\pm)$. These approximate power laws are calculated based on different intervals in $\overline{P}_\pm$ chosen as ever narrowing slices of that interval in $\overline{P}_\pm$ in which the numerical data lie. The narrowing intervals approach the small and large $\overline{P}_\pm$ limit, respectively. With these power law approximations for different intervals in $\overline{P}_\pm$ we obtain a series of approximate integrals for those intervals, for which due to practical limitations there are no numerical data (for small and large values of $\overline{P}_\pm$), and take the limit. This enables us to carry out the integral in Eq. (24) numerically for the whole range from $\overline{P}_\pm = 0$ to $\overline{P}_\pm = \infty$.

This integration leads to the universal amplitudes $\overline{\Gamma}_\pm(\gamma)$ as shown in Fig. 10. For small opening angles

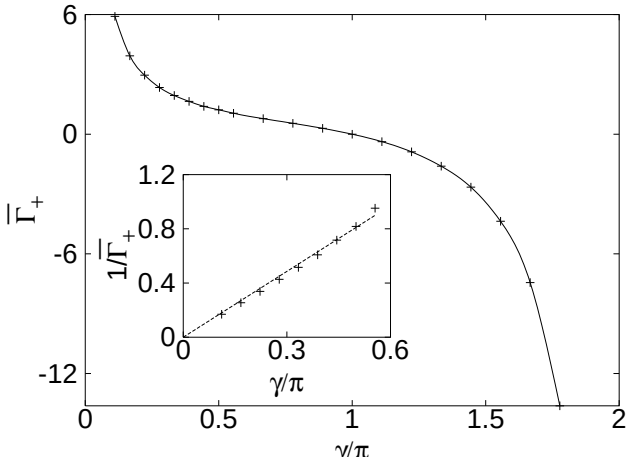

FIG. 10: The amplitude of the line contribution to the excess adsorption for $t > 0$ [Eqs. (14) and (15)] as a function of the opening angle γ. The full line is a fit through the data (+). The inset shows that over a wide range $\overline{\Gamma}_+(\gamma) \approx 1.62/(\gamma/\pi)$. $\overline{\Gamma}_+(\pi) = 0$ by definition. Note that $\overline{\Gamma}_+(\gamma) < |\overline{\Gamma}_+(2\pi - \gamma)|$.

γ they diverge as $\overline{\Gamma}_\pm(\gamma \to 0) \sim 1/\gamma$, vary linearly close to $\gamma = \pi$ for $\gamma \leq \pi$, and their absolute values increase rapidly for $\gamma > \pi$. Numerical evidence suggests that this latter increase is exponential (but no divergence [see Fig. 11]).

Strikingly, the reduced excess adsorption $\overline{\Gamma}_+(\gamma)$ above the critical temperature appears to be proportional to the reduced excess adsorption $\overline{\Gamma}_-(\gamma)$ below the critical temperature. We have calculated their ratio for seven

opening angles ranging from 20° to 240° and found

$$\overline{\Gamma}_+(\gamma)/\overline{\Gamma}_-(\gamma) = 1.137 \pm 0.006, \tag{25}$$

i.e., their ratio appears to be independent of γ.

Ratios of the amplitudes of the excess adsorption above and below T_c have been investigated for the case of a planar wall theoretically [8], experimentally [7], and using Monte Carlo simulations [9]. The values obtained experimentally for the ratios of the amplitudes for the planar case (mean value: 1.19 ± 0.04) agree rather well with the result of the Monte Carlo simulations (1.11); the corresponding mean field value is $1/\sqrt{2}$ [8].

The angular dependence of the reduced excess adsorption shows that for large angles, i.e., for a ridge, the absolute values are larger than for small angles, i.e., for a wedge: $\overline{\Gamma}_\pm(\gamma) < |\overline{\Gamma}_\pm(2\pi - \gamma)|$. One can calculate the excess adsorption at a periodic array of wedges and ridges (see, c.f., Fig. 13) if their edges are sufficiently far apart from each other so that their influences do not interfere (see part B of the Appendix). The result expressed by Eq. A.5 in the Appendix shows that in this limiting case the line contribution to the excess adsorption, which captures the effect of the wedges and ridges, is the sum of the contributions of single wedges of opening angle γ_w and of single ridges of opening angle $\gamma_r = 2\pi - \gamma_w$ sharing the same temperature dependence $|t|^{\beta-2\nu}$. Thus the amplitude $\overline{\Gamma}_\pm^{wr}$ of the combined contribution of one wedge and a neighboring ridge forming the basic building block of the array is given as as $\overline{\Gamma}_\pm^{wr} = \overline{\Gamma}_\pm(\gamma_w) + \overline{\Gamma}_\pm(\gamma_r)$. This quantity may be viewed as a function of $\gamma_r - \gamma_w = 2\pi - 2\gamma_w = 2(\pi - \gamma_w)$, which characterizes the roughness of the surface. $\overline{\Gamma}_+^{wr}(\gamma_r - \gamma_w)$ is plotted in Fig. 11 for $(t > 0)$. One can see that all values are negative, i.e., the total excess adsorption (relative to a planar substrate with the same area as the actual one of the corrugated surface) is decreased by the line contribution. This demonstrates that the decrease in adsorption for a ridge with $\gamma_r = 2\pi - \gamma_w$ dominates the increase due to the corresponding wedge with opening angle γ_w (see Fig. 10). The amplitude $\overline{\Gamma}_+^{wr}$ varies quadratically for small roughness and exponentially for large roughness.

In Ref. [28] the total excess adsorption has been calculated for curved surfaces. For a curved membrane with both sides exposed to a fluid near criticality, the sum of the excess adsorptions on the two sides per unit area was found to be larger for spherical regions of the membrane and smaller for cylindrical regions as compared to that for flat regions. Since the cylindrical regions may be viewed as rounded wedges and ridges, this latter finding exhibits the same qualitative trend as found here for the periodic array of wedges and ridges.

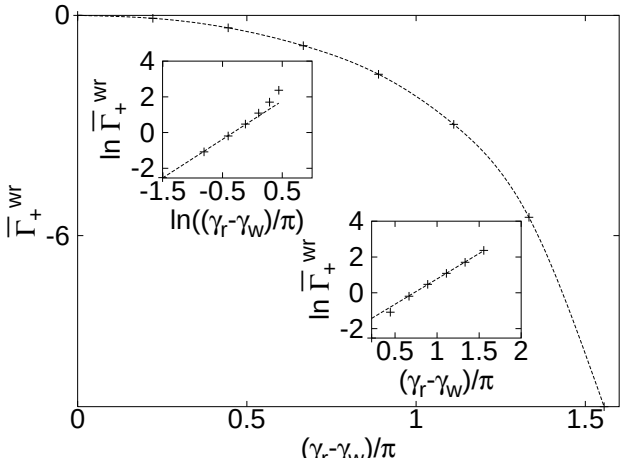

FIG. 11: The amplitude $\overline{\Gamma}_+^{wr}$ of the line contribution to the excess adsorption of the basic unit of one wedge of opening angle γ_w and one ridge of opening angle $\gamma_r = 2\pi - \gamma_w$ in an array of effectively independent wedges and ridges as a function of $(\gamma_r - \gamma_w)/\pi$, which characterizes the roughness of the surface (see, c.f., Fig. 13). The dashed lines are fits. The insets show the behaviors in the limiting cases on a log-log scale and a log-linear scale for small and large roughness, respectively. They indicate that $\overline{\Gamma}_+^{wr}((\gamma_r - \gamma_w) \to 0) \sim (\gamma_r - \gamma_w)^2$ and that $\overline{\Gamma}_+^{wr}$ increases as $exp\{[(\gamma_r - \gamma_w)/\pi]^3\}$ up to $(\gamma_r - \gamma_w)/\pi = 2$.

IV. FREE ENERGY OF THE CONFINED FLUID AND CASIMIR TORQUE

In the previous chapters we have investigated structural properties, i.e., order parameter profiles of critical fluids in wedges and close to ridges. In the followings we comment on their thermodynamic properties based on the free energy of such systems.

The volume $V(\gamma)$ of the system shown in, c.f., Fig. 12 (for another possible choice see, c.f., Fig. 14) is bounded by the walls of the wedge or ridge, which in turn end in the linear edge forming the vertex. Accordingly in the thermodynamic limit the total free energy F decomposes into a bulk, a surface, and a line contribution:

$$F(T;\gamma) = V(\gamma) f_b(T) + S f_s(T) + L f_l(T,\gamma), \tag{26}$$

where $f_b(T)$ is the bulk free energy density, $f_s(T)$ is the surface free energy density, and $f_l(T,\gamma)$ is the line free energy density. S is the total surface area of the wall in contact with the fluid, L is the length of the edge. Each of the three terms in the free energy and thus the total free energy itself are sums of a singular part $(f_{sing}^{(b,s,l)}(t,\gamma))$, which contains the thermodynamic singularities in the vicinity of the bulk critical point $t = (T - T_c)/T_c \to 0$, and an analytic background contribution $(f_{back}^{(b,s,l)}(T,\gamma))$.

The leading singular part of the total free energy can

be written in the form (see, e.g., Refs. [5], [46], and [47]):

$$\frac{F^{\pm}_{sing}(t,\gamma)}{k_BT_c} = \frac{V(\gamma)}{(\xi_0^{\pm})^d}\left(-\frac{a_b^{\pm}}{\alpha(1-\alpha)(2-\alpha)}|t|^{2-\alpha}\right) + \frac{S}{(\xi_0^{\pm})^{d-1}}\left(-\frac{a_s^{\pm}}{\alpha_s(1-\alpha_s)(2-\alpha_s)}|t|^{2-\alpha_s}\right) + \frac{L}{(\xi_0^{\pm})^{d-2}}\left(-\frac{a_l^{\pm}(\gamma)}{\alpha_l(1-\alpha_l)(2-\alpha_l)}|t|^{2-\alpha_l}\right). \quad (27)$$

Here $\alpha \simeq 0.11$ is the bulk specific heat exponent, $\alpha_s = \alpha + \nu$, $\alpha_l = \alpha + 2\nu$, and $a_b^{\pm}$ and $a_s^{\pm}$ are universal bulk and surface amplitudes. The bulk contribution depends trivially on γ via the geometry $V(\gamma)$, whereas the surface contribution is independent of γ. The line contribution carries a nontrivial dependence on γ via the universal amplitude functions $a_l^{\pm}(\gamma)$.

The background contribution takes on the form

$$\frac{F^{\pm}_{back}(T,\gamma)}{k_BT_c} = \frac{V(\gamma)}{(\xi_0^{\pm})^d}f^{(b)}_{back}(T) + \frac{S}{(\xi_0^{\pm})^{d-1}}f^{(s)}_{back}(T) + \frac{L}{(\xi_0^{\pm})^{d-2}}f^{(l)}_{back}(T,\gamma). \quad (28)$$

If one of the sidewalls is moveable around the vertex with the far end suspended at, say, a force microscope, the torque

$$M = -\frac{\partial F(T;\gamma)}{\partial \gamma} \quad (29)$$

exerted by the fluid in the wedge or ridge on its sidewalls is experimentally accessible:

$$\frac{M^{\pm}}{k_BT_c} = -\frac{\partial V(\gamma)}{\partial\gamma}(\xi_0^{\pm})^{-d}\left(-\frac{a_b^{\pm}}{\alpha(1-\alpha)(2-\alpha)}|t|^{2-\alpha} + f^{(b)}_{back}(T)\right) - L(\xi_0^{\pm})^{-(d-2)}\left(-\frac{\partial a_l^{\pm}(\gamma)/\partial\gamma}{\alpha_l(1-\alpha_l)(2-\alpha_l)}|t|^{2-\alpha_l} + \frac{\partial f^{(l)}_{back}(T,\gamma)}{\partial\gamma}\right). \quad (30)$$

With the bulk contribution known independently, this measurement provides access to the universal amplitude functions $a_l^{\pm}(\gamma)$ by focusing on the thermal singularity $\sim |t|^{2-\alpha_l} = |t|^{\nu} = |t|^{0.63}$ in $d = 3$, since $d\nu = 2 - \alpha$. The singular contribution to M can be called a critical Casimir torque. For fluids information about the background term can be obtained from Eq. (A7) in Ref. [48] and from Refs. [49, 50, 51].

Within mean-field theory $2 - \alpha_l = 1$ so that the singular line contribution becomes indistinguishable from the analytical background contribution. Thus our present approach renders only the sum of these two contributions without the possibility to isolate the amplitude functions $a_l^{\pm}(\gamma)$. As indicated by the pole $\sim \frac{1}{1-\alpha_l}$ for $d \to 4$, inclusion of Gaussian fluctuations beyond the simple mean-field theory is expected to generate a term $\sim t\ln|t|$ due to the resonance of the singular contribution $\sim \frac{1}{1-\alpha_l}t^{2-\alpha_l}$ with an analytical background term $\sim t$ [52]. The amplitude of the singular term $\sim t\ln|t|$ would allow one to retrieve at least the mean-field expression for $a_l^{\pm}(\gamma)$. However, this technically challenging inclusion of Gaussian fluctuations is beyond the scope of the present work.

A suitable approach to obtain the change of the free energy upon varying the opening angle of the wedge or ridge involves calculating the field theoretical stress tensor. Analogously to the free energy density, the corresponding torque requires additive renormalization up to second order in temperature [53]. We have followed this route within the present mean-field theory without isolating the critical Casimir torque. We have found that this combined torque diverges as $M \sim 1/\gamma^2$ for small γ, and it appears to be a linear function of $1/\gamma^2$ within the angle range between $\gamma = 20°$ and $\gamma = 280°$.

V. SUMMARY

In the present study of critical adsorption in wedges and close to ridges (see Fig. 1) we have obtained the following main results:

(1) We have discussed the scaling properties of the order parameter profile $m_{\pm}(\boldsymbol{r}, t;\gamma) = a|t|^{\beta}P_{\pm}(r/\xi_{\pm},\theta;\gamma)$ in terms of the bulk correlation length $\xi_{\pm} = \xi_0^{\pm}|t|^{-\nu}$ above and below the critical point T_c with $t = (T - T_c)/T_c$. The universal scaling functions $P_{\pm}(r/\xi_{\pm},\theta;\gamma)$ diverge according to a power law close to the walls of the wedge or ridge, and decay exponentially far away from the walls [Eq. (8)].

(2) In the thermodynamic limit the excess adsorption $\tilde{\Gamma}_{\pm}(s_{\perp}, s_{\parallel}, t;\gamma)$ [Eq. (10)] for volumes with linear extensions $s_{\perp}$ and $s_{\parallel}$ (see Figs. 12 and 14) decomposes into a surface contribution that scales with the actual surface area of the confining walls $(s_{\perp}s_{\parallel}^{(d-2)})$ and a line contribution that scales with the extension in the invariant directions $(s_{\parallel}^{(d-2)})$ [see Eq. (11)] as described in detail in the Appendix. The line contribution is the specific contribution arising from the influence of the edge on the

order parameter profile. Its amplitude $\Gamma_l^{\pm}(t,\gamma)$ has the scaling form $\Gamma_l^{\pm}(t,\gamma) = a\xi_0^{\pm 2}|t|^{\beta-2\nu}\overline{\Gamma}_{\pm}(\gamma)$ with the universal amplitude functions $\overline{\Gamma}_{\pm}(\gamma)$ [Eq. (15)] carrying the dependence on the opening angle γ.

(3) We calculate the above scaling functions within mean-field theory [see Eqs. (16) and (17)] using a numerical algorithm both above and below the critical temperature (for a wedge see Figs. 2-5, for a ridge see Figs. 7 and 8). The amplitude functions of the power law divergence of the profile close to the walls [Eq. (8)] are shown in Fig. 6.

(4) Our numerical calculation also yields the experimentally relevant excess adsorption within mean-field approximation. The universal amplitudes $\overline{\Gamma}_+(\gamma)$ are shown in Fig. 10. For small opening angles γ they diverge as $\overline{\Gamma}_+(\gamma \to 0) \sim 1/\gamma$, vary linearly close to $\gamma = \pi$ for $\gamma \leq \pi$, and their absolute values increase rapidly for $\gamma > \pi$. Numerical evidence suggests that this latter increase is exponential, but without divergence [see Fig. 11]. The reduced excess adsorption $\overline{\Gamma}_+(\gamma)$ above the critical temperature appears to be proportional to the reduced excess adsorption $\overline{\Gamma}_-(\gamma)$ below the critical temperature with $\overline{\Gamma}_+(\gamma)/\overline{\Gamma}_-(\gamma) = 1.137 \pm 0.006$. We have considered a wedge and a ridge together as forming the basic unit in a periodic array (see Fig. 13). The total excess adsorption relative to that of a planar substrate with the same area as the actual one of the corrugated surface [Eq. (A.6)] is decreased by the line contribution (see Fig. 11).

(5) The variation of the free energy of the system with the opening angle of the wedge or ridge gives rise to a torque acting on the sidewalls [Eq. (29)]. The free energy decomposes into a singular contribution exhibiting scaling [see Eq. (27)], and an analytic background contribution [Eq. (28)]. In $d = 3$ the critical Casimir torque varies as $a_l^{\pm}(\gamma)|t|^{\nu}$ with universal amplitude functions $a_l^{\pm}(\gamma)$. This cusplike temperature singularity is expected to be experimentally accessible via suitable force microscopy. The theoretical calculation of the corresponding amplitude functions remains as a challenge.

Acknowledgments

G. P. is indebted to F. Schlesener and M. Krech for many helpful discussions that settled numerous technical and physical questions.

APPENDIX: DECOMPOSITION OF THE EXCESS ADSORPTION

In this appendix we discuss how the excess adsorption in a wedge or at a ridge decomposes into surface and line contributions [see Eqs. (11)-(13)]. In the definition of the excess adsorption [Eq. (10)] one considers a finite volume V of integration that is enlarged to fill the total volume of the wedge or ridge in the thermodynamic limit. As shown below for two examples, the expression for the line term (such as Eq. (13)) actually depends on the choice of the shape of the volume V.

In the following we first analyze the excess adsorption for a single macroscopic wedge or ridge (1), which will be followed by a discussion of the excess adsorption for two possible experimental realizations (2 and 3).

1. A single macroscopic wedge or ridge

a. First choice of the volume of integration

Our first choice for V is shown in Fig. 12 for the case of a wedge. This choice is inspired by the idea that the single wedge or ridge considered here is ultimately a member of a periodic array. With this polygonal cross section and a similarly constructed one for the ridge, one can cover the total volume V_{tot} of a fluid in contact with a surface formed as a periodic array of wedges and ridges in a natural way (see Fig. 13). All the formulas explicitly stated below for the wedge are valid for the ridge, too.

The volume V is symmetric with respect to the bisector plane of the wedge, which allows us in the following

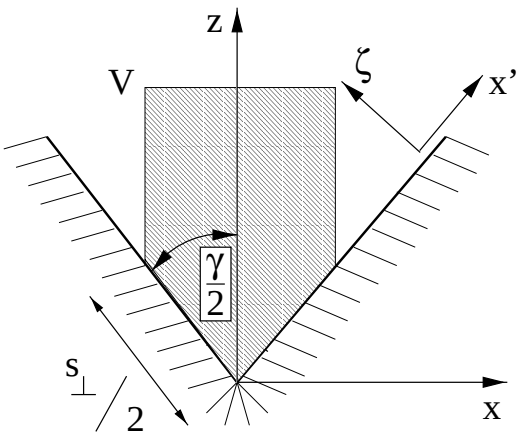

FIG. 12: One choice for the volume V of integration in the definition of the excess adsorption [Eq. (10)] with its cross section in the plane perpendicular to the invariant directions.

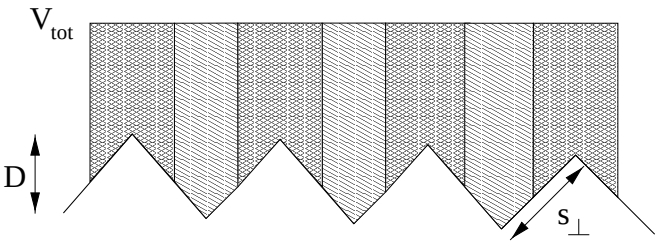

FIG. 13: A fluid is bounded by a substrate shaped as a periodic array of wedges and ridges with a finite depth D. The total volume of the fluid V_{tot} can be naturally decomposed into subvolumes of the type shown in Fig. 12.

to consider only one half of the wedge, and multiply the corresponding expression by a factor of two.

As indicated in Fig. 12 the volume V in Eq. (10) is finite and thus the integral is finite, too. As a first step in carrying out the thermodynamic limit we keep the shape of V but shift the upper boundary $z = const$ to infinity. Since $m_\pm$ approaches m_b exponentially, this extension of V increases $\tilde{\Gamma}_\pm$ by an exponentially small amount and thus does not contribute to the two leading terms under consideration in Eq. (11). (In the spirit of the thermodynamic limit one first increases V before one can possibly consider the limit $t \to 0$. Therefore these arguments are not impaired by a power law decay of $m_\pm(z \to \infty, t = 0)$ in the thermodynamic limit.) For the resulting semi-infinite strip Eq. (10) can be rewritten in the following form by adding and subtracting the order parameter profile $m_\pm^{\infty/2}(\zeta = r\sin\theta, t)$ of a fluid in contact with an infinite planar wall in the integrand (see Figs. 1 and 12):

$$\begin{aligned}\tilde{\Gamma}_\pm(s_\perp, s_\parallel, t; \gamma) \;=\; & 2s_\parallel^{d-2} \int_0^\infty d\zeta \int_{\frac{\zeta}{\tan(\gamma/2)}}^{\frac{s_\perp}{2}+\frac{\zeta}{\tan(\gamma/2)}} dx' [m_\pm(r(x',\zeta),\theta(x',\zeta),t;\gamma) - m_\pm^{\infty/2}(\zeta,t)] \\ & + 2s_\parallel^{d-2} \int_0^\infty d\zeta \int_{\frac{\zeta}{\tan(\gamma/2)}}^{\frac{s_\perp}{2}+\frac{\zeta}{\tan(\gamma/2)}} dx' [m_\pm^{\infty/2}(\zeta,t) - m_b(t)] \qquad \text{(A.1)}\end{aligned}$$

where $x' = r\cos\theta = z\cos(\gamma/2) + x\sin(\gamma/2)$ is the coordinate measured from the apex parallel to the nearest wall of the wedge and $\zeta = r\sin\theta = z\sin(\gamma/2) - x\cos(\gamma/2)$ is the normal distance from the nearest wall of the wedge (see Fig. 12).

In the inner integral of the first term the upper integration limit can be shifted to infinity, i.e., $s_\perp \to +\infty$, with an addition of only exponentially small corrections to the integral, because $m_\pm$ approaches $m_\pm^{\infty/2}$ exponentially for $x' \to +\infty$ at fixed ζ. Thus the first term in Eq. (A.1) approaches a constant for $s_\perp \to +\infty$ and this constant involves an unlimited integral over the whole half of the wedge. Expressed in terms of cylindrical coordinates this term yields the line contribution $\Gamma_l^\pm(t,\gamma) s_\parallel^{(d-2)}$ in Eqs. (11) and (13).

As the integrand of the second term in Eq. (A.1) does not depend on x', the inner integration simply yields a factor $s_\perp/2$. The outer integral then yields $\Gamma_\pm^{\infty/2}$ in Eq. (3). Together with Eq. (12) this verifies Eq. (11).

b. *Second choice of the volume of integration*

Our second choice of the shape of the volume V as shown in Fig. 14(a) corresponds to the one used in Ref. [37], where liquids confined by two opposing structured walls have been studied; in this geometry one cannot infinitely extend the volume in the $+z$ direction. On the other hand in the case of the ridge as shown in Fig. 14(b), starting out from a finite volume V, the upper boundary of the volume ($z = const$) can be shifted to $+\infty$ as well as the two vertical boundaries ($x = \pm const$) to $\pm\infty$ with only exponentially small corrections to the integral in Eq. (10), because in the directions $z \to \infty$ and $x \to \pm\infty$ for z fixed the order parameter attains its bulk value exponentially. As for the previous choice also for the present geometries Eq. (10) can be rewritten by adding and subtracting the order parameter profile $m_\pm^{\infty/2}(\zeta = r\sin\theta, t)$ of a fluid in contact with an infinite

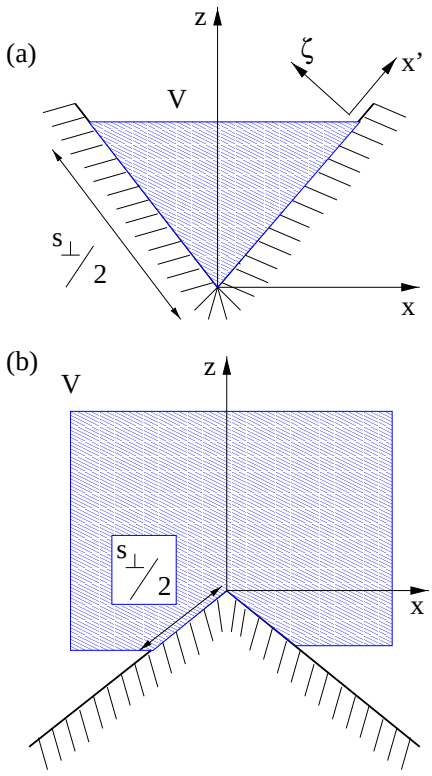

FIG. 14: A second choice for the volume V of integration in the definition of the excess adsorption [Eq. (10)] for a wedge (a) and a ridge (b) with its cross section in the plane perpendicular to the invariant directions.

planar wall in the integrand (see Fig. 14):

$$\tilde{\Gamma}_{\pm}(s_\perp, s_\parallel, t; \gamma) = 2s_\parallel^{d-2} \int_0^{\frac{s_\perp}{4}\sin\gamma} d\zeta \int_{\frac{\zeta}{\tan(\gamma/2)}}^{\frac{s_\perp}{2}-\zeta\tan(\gamma/2)} dx' [m_\pm(r(x',\zeta),\theta(x',\zeta),t;\gamma) - m_\pm^{\infty/2}(\zeta,t)] + 2s_\parallel^{d-2} \int_0^{\frac{s_\perp}{4}\sin\gamma} d\zeta \int_{\frac{\zeta}{\tan(\gamma/2)}}^{\frac{s_\perp}{2}-\zeta\tan(\gamma/2)} dx' [m_\pm^{\infty/2}(\zeta,t) - m_b(t)] \quad \text{(A.2)}$$

where as before $x' = r\cos\theta$ is the coordinate parallel to the wall, and $\zeta = r\sin\theta$ normal to it [see Fig. 14(a)]. In the first term the upper integration limits of both integrals can be shifted to infinity, i.e., $s_\perp \to \infty$, with an addition of only exponentially small corrections to the integral, because $m_\pm$ approaches $m_\pm^{\infty/2}$ exponentially for $x' \to +\infty$ at fixed ζ, and $m_\pm$ attains its bulk value exponentially for $\zeta \to +\infty$ at fixed x'. Thus for the first term the limit $s_\perp \to \infty$ exists and is finite with the two-dimensional integral covering the whole half of the wedge. Expressed in terms of cylindrical coordinates this term yields the line term $\Gamma_l^\pm(t,\gamma) s_\parallel^{(d-2)}$ [see Eqs. (11) and (13)] as for the previous choice of the volume.

The inner integral in the second term can be carried out, because the integrand is independent of x'. This yields a prefactor $\frac{s_\perp}{2} - \zeta\left[\tan\frac{\gamma}{2} + \frac{1}{\tan\gamma/2}\right] = \frac{1}{2}\left\{s_\perp - \frac{4}{\sin\gamma}\zeta\right\}$. The first term of this prefactor gives rise to the surface contribution in Eqs. (3), (11), and (12), if one shifts the upper integration limit of the ζ integration to infinity with the addition of exponentially small corrections. After multiplying this prefactor by two, its second term gives rise, however, to another line contribution with the amplitude

$$\hat{\Gamma}_l^\pm(t,\gamma) = \frac{-4}{\sin\gamma} \int_0^\infty \zeta [m_\pm^{\infty/2}(\zeta,t) - m_b(t)] d\zeta, \quad \text{(A.3)}$$

where the upper limit of integration has also been shifted to infinity with an exponentially small correction. We note that this additional line term depends on the order parameter profile at a planar substrate only. Due to the extra factor ζ in the integrand, the integral in Eq. (A.3) is finite for $d = 4$ in spite of $m_\pm^{\infty/2}(\zeta \to 0) \sim \zeta^{-1}$ in this case, i.e., $\hat{\Gamma}_\pm$ does not carry a factor proportional to $\frac{1}{\nu-\beta}$ as $\Gamma_\pm^{\infty/2}$ does (compare Eq. (6)).

Thus in the thermodynamic limit the two choices of the integration volume V yield the same surface contributions $\Gamma_s^\pm$ to the excess adsorption but different subdominant line contributions $\Gamma_l^\pm$:

$$\int_V d^d x\, m_\pm(\boldsymbol{x}) = V m_b + S\Gamma_s^\pm + L\Gamma_l^\pm + \mathcal{O}(s_\perp^{-1}) \quad \text{(A.4a)}$$

with

$$\Gamma_l^\pm = \Gamma_{l,I}^\pm(t,\gamma) = 2\int_0^{\gamma/2} d\theta \int_0^\infty dr\, r [m_\pm(r,\theta,t;\gamma) - m_\pm^{\infty/2}(\zeta(r,\theta),t)], \quad \text{choice I,} \quad \text{(A.4b)}$$

and

$$\Gamma_l^\pm = \Gamma_{l,II}^\pm(t,\gamma) = \Gamma_{l,I}^\pm(t,\gamma) + \hat{\Gamma}_l^\pm(t,\gamma), \quad \text{choice II,} \quad \text{(A.4c)}$$

with $S = s_\perp s_\parallel^{d-2}$, $L = s_\parallel^{d-2}$, and $\hat{\Gamma}_l^\pm$ given by Eq. (A.3). Experiments cannot be carried out for infinitely deep wedges. Instead they can be carried out for either a periodic array of wedges or for a single wedge of finite depth carved out from a wide planar surface. In both cases additional ridges must be formed giving rise to their own adsorption properties. Therefore experiments on such systems give access only to certain combinations of wedge and ridge excess adsorptions, whose corresponding line contributions carry the relevant additional information about the nonplanar substrate geometry. The actual choice of the corresponding integration volume depends on the actual experimental setup (compare, e.g., Fig. 13; see Subsecs. 2 and 3) The results of this subsection show that the line contributions depend on such details even in the thermodynamic limit.

2. Periodic array of wedges and ridges

In this subsection we consider a substrate with a periodic series of edges and wedges as depicted in Fig. 13. There is a variety of experimental techniques to create such kind of surface morphology. If the opening angle of the wedges is γ, the opening angle of the ridges is $2\pi - \gamma$. Here we focus on the limiting case that the depth of the wedges $D = s_\perp \cos(\gamma/2)$ is sufficiently large, so that the deviations of the profiles close to the edges of the wedges and ridges, respectively, from the profile of a fluid exposed to an infinite planar substrate do not influence each other. As apparent from Figs. 12 and 13, this case corresponds to the first choice of the volume of integra-

tion for the single wedge or ridge and thus leads to the following decomposition of the excess adsorption [see Eq. (A.4b)]

$$\int_{V_{tot}} d^d x\, m_\pm(\boldsymbol{x},t;\gamma) = V_{tot} m_b(t) + S_{tot}\Gamma_s^\pm(t) + L(N_w\Gamma_{lw}^\pm(t,\gamma_w) + N_r\Gamma_{lr}^\pm(t,\gamma_r)) + \mathcal{O}(s_\perp^{-1}) \quad \text{(A.5)}$$

with the total surface of the substrate $S_{tot} = N s_\perp s_\parallel^{d-2}$, where $N = N_w + N_r$ is the number of segments of length $s_\perp$, $\Gamma_s^\pm(t) = \Gamma_\pm^{\infty/2}(t)$ [see Eq. (3)], $L = s_\parallel^{d-2}$, $N_w = N_r$ are the numbers of wedges and ridges, respectively, and

$$\Gamma_{lw(r)}^\pm(t,\gamma_{w(r)}) = 2\int_0^{\gamma_{w(r)}/2} d\theta \int_0^\infty dr\, r[m_\pm^{w(r)}(r,\theta,t;\gamma_{w(r)}) - m_\pm^{\infty/2}(\zeta(r,\theta),t)], \quad \text{(A.6)}$$

where γ_w is the opening angle of the wedge, and $\gamma_r = 2\pi - \gamma_w$. This is in accordance with Eqs. (32)-(36) of Ref. [37], where a different coordinate system was used [54].

3. A single wedge embedded into a planar wall

In this subsection we consider a single wedge of opening angle γ carved out of a planar surface, thus producing also two ridges of opening angles $(3\pi-\gamma)/2$ (see Fig. 15). Due to the symmetry of the configuration we consider

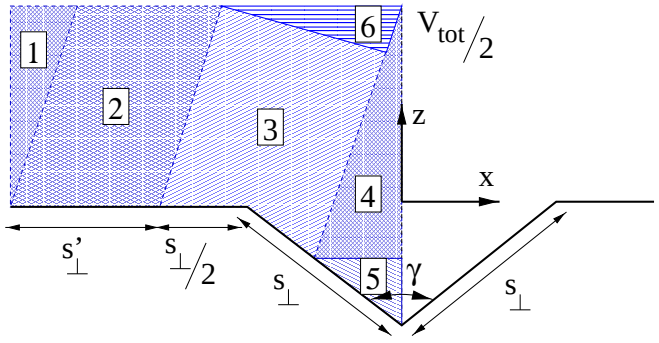

FIG. 15: A fluid is bounded by a substrate shaped as a wedge carved out of an infinite planar wall. The total volume of the fluid can be decomposed into the numbered subvolumes that emerge naturally due to subvolumes 3 and 5 used for describing a single ridge (first choice of the volume of integration (1 a)) and a single wedge (second choice of the volume of integration (1 b)), respectively.

only half of the wedge and focus on the case that $s_\perp$ is sufficiently large so that the ridges and the wedge do not influence each other. One half of the total volume of the fluid is decomposed into six numbered subvolumes as shown in Fig. 15. We calculate the excess adsorption [Eq. (10)] separately for each one of the subvolumes by adding and subtracting the profile of a fluid exposed to an infinite planar wall $m_\pm^{\infty/2}$ in the integral of the order parameter as in Subsecs. 1 and 2.

For the first volume there is no line contribution resulting from the integral over the difference of the actual profile $m_\pm$ from that in front of an infinite planar wall $m_\pm^{\infty/2}$, because this difference is exponentially small in the thermodynamic limit. There is also no surface term, because this first volume touches the substrate only at one point. However, following similar considerations as for a single wedge or ridge, this volume gives rise to a line contribution [see Eq. (A.4a)] to the excess adsorption [Eq. (10)] due to the deviation of $m_\pm^{\infty/2}$ from m_b with amplitudes:

$$\hat\Gamma_{l,1}^\pm(t,\gamma) = \tan\frac{\pi-\gamma}{4}\int_0^\infty \zeta[m_\pm^{\infty/2}(\zeta,t) - m_b(t)]d\zeta, \quad \text{(A.7)}$$

where we have shifted the $z = const$ boundary to $+\infty$ with an exponentially small correction to the integral.

In the thermodynamic limit ($s_\perp,\ s'_\perp \to \infty$) the adsorption profile $m_\pm$ in the second volume will tend exponentially to that of a fluid exposed to an infinite planar wall $m_\pm^{\infty/2}$. Thus it supplies a surface term with the amplitudes $\Gamma_s^\pm(t) = \Gamma_\pm^{\infty/2}(t)$ [see Eq. (3)] for the area $s'_\perp s_\parallel^{d-2}$ We note that this subvolume two when extended to infinity in the $+z$ direction overlaps with the other half of the wedge, but this results in only an exponentially small correction to the excess adsorption, because the profile $m_\pm$ approaches the bulk value m_b exponentially with the distance ζ from the wall. The subvolume two does not generate a line contribution.

The third volume gives the same contributions [Eq. (A.4a)] to the excess adsorption as a single ridge of opening angle $(3\pi-\gamma)/2$ with the first choice of volume of integration shown in Fig. 12, i.e., a surface term with the amplitudes $\Gamma_s^\pm(t) = \Gamma_\pm^{\infty/2}(t)$ for an area $s_\perp s_\parallel^{d-2}$ [see Eq. (3)] and line term amplitudes $\Gamma_{lr}^\pm(t,\gamma_r = (3\pi-\gamma)/2)$ [see Eq. (A.6)]. Note that the volume of integration can be extended to infinity in the direction parallel to the bisector of the ridge even though in this case there is an overlap with the other half of the wedge, because this results in only an exponentially small correction to the excess adsorption as the profile $m_\pm$ approaches the bulk value

m_b exponentially in this direction further away from the ridge.

Similarly to subvolume one, subvolume four does not generate a line term resulting from the integral over the difference of the actual profile $m_\pm$ from $m_\pm^{\infty/2}$. There is also no surface term, but similar considerations as for a single wedge or ridge show that this subvolume gives rise to a line contribution to the excess adsorption with amplitudes of the form:

$$\hat{\Gamma}_{l,4}^{\pm}(t,\gamma) = \left[\tan\frac{\pi-\gamma}{4}+\tan\frac{\gamma}{2}\right] \times\int_0^\infty \zeta[m_\pm^{\infty/2}(\zeta,t)-m_b(t)]d\zeta, \quad \text{(A.8)}$$

once we have shifted the $x=0$ boundary to $+\infty$ with an exponentially small correction to the integral.

The fifth subvolume together with its counterpart at $x>0$ gives the same contributions [Eq. (A.4c] to the excess adsorption as a wedge of opening angle γ with the second choice of the volume of integration shown in Fig. 14(a), i.e., a surface term with amplitudes $\Gamma_s^\pm(t)=\Gamma_\pm^{\infty/2}(t)$ [see Eq. (3)] for the area $s_\perp s_\parallel^{d-2}$, and the line term amplitudes $\Gamma_{l,II}^\pm(t,\gamma)$ from Eq. (A.4c).

Finally the subvolume six yields only an exponentially small contribution to the excess adsorption.

Adding up all contributions to the excess adsorption in this geometry one obtains

$$\int_{V_{tot}} d^dx\, m_\pm(\boldsymbol{x},t;\gamma) = V_{tot}m_b(t)+S_{tot}\Gamma_s^\pm(t)+L\Big[\Gamma_{lw}^\pm(t,\gamma_w)+2\Gamma_{lr}^\pm(t,\gamma_r=(3\pi-\gamma_w)/2) +4\left(\frac{1}{\cos\frac{\gamma_w}{2}}-\frac{1}{\sin\gamma_w}-\frac{1}{2}\tan\frac{\gamma_w}{2}\right)\int_0^\infty\zeta[m_\pm^{\infty/2}(\zeta,t)-m_b(t)]d\zeta\Big]+\mathcal{O}(s_\perp^{-1}). \quad \text{(A.9)}$$

As in the case of a periodic array of wedges and ridges the line contribution to the excess adsorption contains a combination of wedge and ridge terms. Since different combinations thereof enter into the excess adsorption of a periodic array and of a single embedded wedge, measurements of both of them provide independent information. However, these configurations do not allow one to access the ridge and wedge contributions individually. In the case of a single embedded wedge the line contribution to the excess adsorption contains in addition the first moment of the order parameter profile of a semi-infinite planar system, which can be determined independently from the knowledge of $m^{\infty/2}(\zeta)$.

[1] J. Zinn-Justin, *Quantum Field Theory and Critical Phenomena* (Oxford University Press, Oxford, 1989).

[2] K. Binder and P. C. Hohenberg, Phys. Rev. B **6**, 3461 (1972); **9**, 2194 (1974).

[3] M. E. Fisher and P.-G. de Gennes, C. R. Acad. Sci. B **287**, 207 (1978).

[4] K. Binder, in *Phase Transitions and Critical Phenomena*, edited by C. Domb and J. L. Lebowitz (Academic, London, 1983), Vol. 8, p. 1.

[5] H. W. Diehl, in *Phase Transitions and Critical Phenomena*, edited by C. Domb and J. L. Lebowitz (Academic, London, 1986), Vol. 10, p. 75.

[6] H. W. Diehl, Int. J. Mod. Phys. B **11**, 3503 (1997).

[7] B. M. Law, Prog. Surf. Sci. **66**, 159 (2001); and references therein.

[8] G. Flöter and S. Dietrich, Z. Phys. B **97**, 213 (1995).

[9] M. Smock, H. W. Diehl, and D. P. Landau, Ber. Bunsenges. Phys. Chem. **98**, 486 (1994).

[10] A. J. Bray and M. A. Moore, J. Phys. A **10**, 1927 (1977).

[11] T. W. Burkhardt and H. W. Diehl, Phys. Rev. B **50**, 3894 (1994).

[12] S. Leibler and L. Peliti, J. Phys. C **30**, L403 (1982), J. Phys. C **16**, 2635 (1983); E. Brézin and S. Leibler, Phys. Rev. B **27**, 594 (1983).

[13] K. Ohno and Y. Okabe, Phys. Rev. B **39**, 9764 (1989).

[14] A. Ciach and H. W. Diehl, Europhys. Lett. **12**, 635 (1990); H. W. Diehl and A. Ciach, Phys. Rev. B **44**, 6642 (1991).

[15] M. E. Fisher and P. J. Upton, Phys. Rev. Lett. **65**, 2402 (1990);**65**, 3405 (1990).

[16] H. W. Diehl and M. Smock, Phys. Rev. B, **47**, 5841 (1993); **48**, 6740 (1993).

[17] B. M. McCoy and T. T. Wu, Phys. Rev. **162**, 436 (1967); *The Two-Dimensional Ising Model* (Harvard University Press, Cambridge, 1973).

[18] J. Wang, D. A. Thompson, and J. G. Simmons, J. Electrochem. Soc. **145**, 2931 (1998); D. W. L. Tolfree, Rep. Prog. Phys. **61**, 313 (1998); Y. Xia and G. W. Whitesides, Annu. Rev. Mater. Sci. **28**, 153 (1998); B. Zhu, J. L. Zhao, and Y. S. Xu, J. Funct. Mater. Devices **7**, 434 (2001); L. J. Lee, M. J. Madou, K. W. Koelling, S. Daunert, S. Lai, C. G. Koh, Y. J. Juang, Y. Lu, and L. Yu, Biomedical Microdevices **3**, 339 (2001).

[19] J. B. Knight, A. Vishwanath, J. P. Brody, and R. H. Austin, Phys. Rev. Lett. **80**, 3863 (1998); M. Grunze, Science **283**, 41 (1999); B. H. Weigl and P. Yager, Science **283**, 346 (1999); P. Gravensen, J. Branebjerg, and O. S. Jensen, J. Micromech. Microeng. **3**, 168 (1993).

[20] J. L. Cardy, J. Phys. A: Math. Gen. **16**, 3617 (1983).
[21] D. B. Abraham and F. Latrémolière, Phys. Rev. E **50**, R9 (1994).
[22] J. L. Cardy, Nucl. Phys. B **240** [FS12], 514 (1984); M. N. Barber, I. Peschel, and P. A. Pearce, J. Stat. Phys. **37**, 497 (1984); T. W. Burkhardt and E. Eisenriegler, J Phys. A **18**, L83 (1985).
[23] M. Pleimling and W. Selke, Eur. Phys. J B **5**, 805 (1998).
[24] A. J. Guttmann and G. M. Torrie, J. Phys. A **17**, 3539 (1984).
[25] F. Iglói, I. Peschel, and L. Turban, Adv. Phys. **42**, 683 (1993).
[26] M. Pleimling, Comp. Phys. Comm. **147**, 101 (2002).
[27] R. Z. Bariev, Sov. Phys. JETP **50**, 613 (1979).
[28] A. Hanke and S. Dietrich, Phys. Rev. E **59**, 5081 (1999).
[29] A. W. Adamson, *Physical Chemistry of Surfaces*, 4th ed. (Wiley, New York, 1982).
[30] A. Hanke, M. Krech, F. Schlesener, and S. Dietrich, Phys. Rev. E **60**, 5163 (1999).
[31] H. B. G. Casimir, Proc. K. Ned. Akad. Wet. **51**, 793 (1948).
[32] M. Krech, *The Casimir Effect in Critical Systems* (World Scientific, Singapore, 1994).
[33] R. Garcia and M. H. W. Chan, Phys. Rev. Lett. **83**, 1187 (1999); Physica B **280**, 55 (2000); J. Low Temp. Phys. **121**, 495 (2000); Phys. Rev. Lett. **88**, 086101 (2002).
[34] M. Krech and S. Dietrich, Phys. Rev. Lett. **66**, 345 (1991); **67**, 1055 (1991); Phys. Rev. A **46**, 1922 (1992); **46**, 1886 (1992); J. Low Temp. Phys. **89**, 145 (1992).
[35] F. Schlesener, A. Hanke, and S. Dietrich, J. Stat. Phys. **110**, 981 (2003).
[36] H. W. Diehl, Ber. Bunsenges. Phys. Chem. **98**, 466 (1994).
[37] M. Schoen and S. Dietrich, Phys. Rev. E **56**, 499 (1997).
[38] F. Schlesener, diploma thesis (U. Wuppertal, 1997).
[39] A. Hanke, F. Schlesener, E. Eisenriegler, and S. Dietrich, Phys. Rev. Lett. **81**, 1885 (1998).
[40] J. H. Carpenter, B. M. Law, and D. S. P. Smith, Phys. Rev. E **59**, 5655 (1999).
[41] A. Hanke and S. Dietrich, Phys. Rev. E **59**, 5081 (1999).
[42] K. Rejmer, S. Dietrich, and M. Napiórkowski, Phys. Rev. E **60**, 4027 (1999).
[43] C. Rascón and A. O. Parry, Nature **407**, 986 (2000).
[44] D. Ross, D. Bonn, and J. Meunier, Nature **400**, 737 (1999).
[45] M. Schoen, Coll. Surf. A **206**, 253 (2002).
[46] S. Dietrich and H. W. Diehl, Z. Phys. B **43**, 315 (1981).
[47] V. Privman, P. C. Hohenberg, and A. Aharony, in *Phase Transitions and Critical Phenomena*, edited by C. Domb and J. L. Lebowitz (Academic, London, 1991), Vol. 14., p. 1.
[48] T. Getta and S. Dietrich, Phys. Rev. E **57**, 655 (1998).
[49] J. R. Henderson, Physica A **305**, 381 (2002).
[50] J. R. Henderson, J. Chem. Phys. **120**, 1535 (2004).
[51] J. R. Henderson, preprint (2004).
[52] V. Privman, Phys. Rev. B **38**, 9261 (1988).
[53] M. Krech and S. Dietrich, Phys. Rev. A **46**, 1886 (1992)
[54] In obtaining the first term in Eq. (34) of Ref. [37], a different scaling of the profile of a fluid exposed to an infinite planar substrate was used as a reference for the wedge and the ridge part, which caused this extra term to appear. If the same scaling is used, as it is correct, this first term becomes zero in accordance with the present findings in Eqs. (A.5) and (A.6).